Applied Numerical Modeling in Geomechanics – 2020 – Billaux, Hazzard, Nelson & Schöpfer (eds.) Paper: 03-11

DEM analysis of reverse fault rupture interaction with rigid foundations

Fernando E. Garcia & Jonathan D. Bray
Department of Civil and Environmental Engineering, University of California, Berkeley, CA, USA

1 INTRODUCTION

Earthquake surface fault rupture is the manifestation of subsurface fault rupture as permanent deformation at the ground surface. As demonstrated by past earthquakes such as the 1999 Kocaeli and Duzce, Turkey, the 1999 Chi-Chi, Taiwan (Bray 2001), and most recently the 2016 Kaikoura, New Zealand earthquakes (Stirling et al. 2017), this phenomenon poses a significant and often devastating hazard in many near-fault regions. While numerous examples exist of the adverse effects earthquake surface fault rupture can have on buildings and infrastructure located near or traversed by active fault traces, there are also many examples of satisfactory building performance in the presence of this hazard (e.g., Bray 2001, Niccum et al. 1976). Case studies of satisfactory building performance set precedent for the use of heavy structures as a means of mitigating damage from earthquake surface fault rupture.

Most studies of the effects of earthquake surface fault rupture on foundations and structures use continuum-based numerical modeling with the finite element method or the finite difference method (e.g., Anastasopoulos et al. 2008, 2010, and Oettle & Bray 2013a,b, 2016). Continuum modeling requires advanced formulations to capture the discontinuity of the shear rupture surface in earthquake surface fault rupture. Furthermore, the soil medium through which fault rupture propagates is often composed of distinct grains of sand or gravel, the effect of which are not easily and not directly captured with finite differences or finite elements. The distinct element method (DEM) is an alternative numerical tool that *directly* models the individual sand grains as distinct particles. Thus, DEM is a useful numerical tool for analyzing fundamental granular influences on earthquake surface fault rupture such as the influence of grain orientation, grain size distribution, and even the amount of void space in between the grains. This study applies DEM to earthquake surface fault rupture and its interaction with a rigid building foundation during reverse fault rupture, also referred to as fault rupture-soil-foundation interaction (FR-SFI). Reverse fault rupture is modeled within a three-dimensional (3D) domain, and the interaction of the propagating fault rupture surface with a rigid foundation is subsequently analyzed. All simulations are performed using the Particle Flow Code in 3D (*PFC3D*, Itasca 2014).

2 DESIGN AND ANALYSIS

Reverse fault rupture is modeled as a 3D boundary-displacement problem in which the rigid-wall boundaries composing the hanging wall move upward quasi-statically in the dip direction. The particles themselves are the same as described in Garcia & Bray (2018a,b). They are rigid clump particles composed of 2 or 3 constituent spheres with a coefficient of uniformity of 1.6 and a median grain diameter (D_{50}) of 2.2 mm. The granular medium contains 148,414 total clumps consisting of 373,858 constituent spheres. The out-of-plane width in the direction of the strike is equal to $10D_{50}$. The out-of-plane boundaries are periodic such that particles that exit one boundary re-enter the domain through the opposite boundary face, and the particles interact across these boundaries. This approximates an infinitely long system in the strike direction.

Further details on the model domain are provided by Garcia & Bray (2018a,b). The lowermost rigid wall boundaries represent the bedrock at which fault rupture through the overlying granular medium initiates.

The boundary conditions of the simulation are modeled after the centrifuge experiments of reverse fault rupture described by Bransby et al. (2008). These experiments were performed with an acceleration due to gravity of 115*g*, making the scaling factor from model to prototype scale $n = 115$. Their model soil height was 130 mm, which is 15 m at the prototype scale. The simulations are set up to mimic the stress distribution within the sandbox spinning in the centrifuge, and the model dimensions are equivalent to those of the sandbox itself rather than the theoretical prototype. Thus, the simulation equivalently has a model height of 130 mm, but rather than applying an equivalent acceleration of 115*g* in the simulation, the particle masses are increased by a factor of 115. This has a similar effect of making the stress distribution within the model equivalent to that in 15 m of homogeneous soil. The contact properties used between particles and particle and foundation in the simulations are the same as those used by Garcia & Bray (2018a,b) for free-field surface fault rupture. The elastic modulus at the contacts is 200 MPa, which is stiff enough to satisfy the assumption of small inter-particle overlaps between contacting particles. Scaling effects are discussed in more detail in Garcia & Bray (2018a) and Garcia & Bray (2019).

The foundation itself in FR-SFI simulations is modeled as a rectangular sphere-cluster composed of several hundred constituent spheres. The length of the foundation in the strike direction is equal to the distance between the periodic boundaries. The foundation is restricted to plane-strain motion so that it approximates an infinitely long strip foundation. Parametric analysis is performed with foundations located at different positions described by Y_0, with contact pressures described by q, and with foundation widths described by B. Y_0 is the in-plane horizontal distance from the bedrock fault location to the center of the foundation. q is the weight of the foundation normalized by its horizontal area.

3 RESULTS AND DISCUSSION

The simulation results highlight the significant influence of foundation contact pressure on the amount of rotation that the foundation undergoes. Figure 1 compares the amount of foundation rotation for different FR-SFI cases and shows a systematic reduction in the amount of in-plane foundation rotation as q increases. This trend applies for each value of Y_0 and B. In general, heavier foundations tend to undergo less rotation during reverse fault rupture than lighter foundations. The significant difference between the cases with Y_0 = -13.2 m and Y_0 = -8.0 m shows that foundation position also significantly affects the interaction between foundation and fault rupture surface, while foundation width appears to have a less significant influence on this interaction.

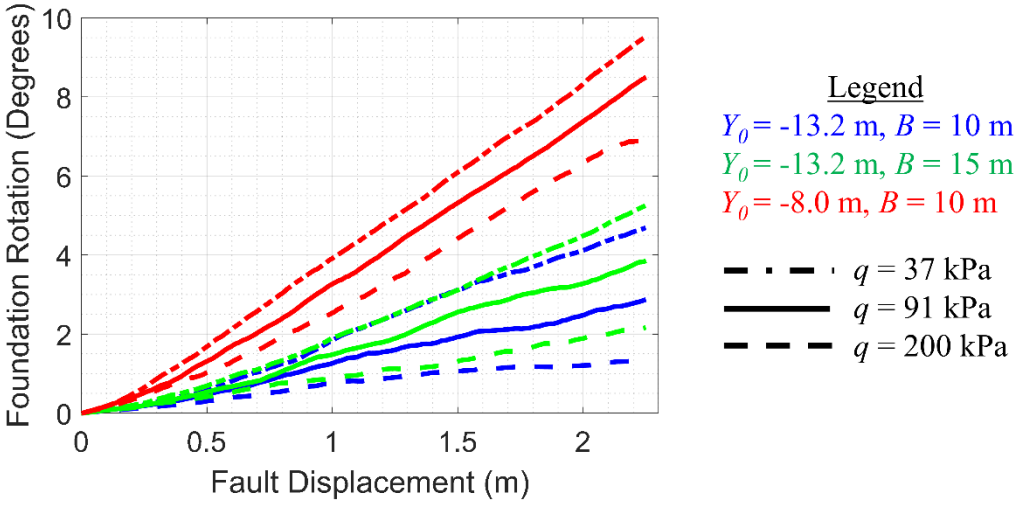

Figure 1. Comparison of in-plane rotations of foundations with different positions, contact pressures, and widths.

The simulation results are presented in terms of clump rotations in Figure 2. High magnitude clump rotations are indicative of high shear activity. The 37 kPa foundation in Figure 2a underwent more rotation than the 200 kPa foundation in Figure 2b because the heavy foundation effectively deflects the path of fault rupture propagation towards the hanging wall side of the foundation. The 37 kPa foundation does not effectively deflect the path of fault rupture propagation, so shear activity occurs beneath the foundation, causing it to rotate more. When B = 15 m in Figure 2c and when Y_0 = -8.0 m in Figure 2d, more shear activity occurs beneath the foundation than seen in Figure 2b. Hence, these foundations undergo more rotation than the 91 kPa, 10 m wide foundation located at Y_0 = -13.2 m due to the increased shear activity beneath the foundation. These findings are consistent with those made by Garcia & Bray (2019), who performed similar simulations with the aid of high-performance computing.

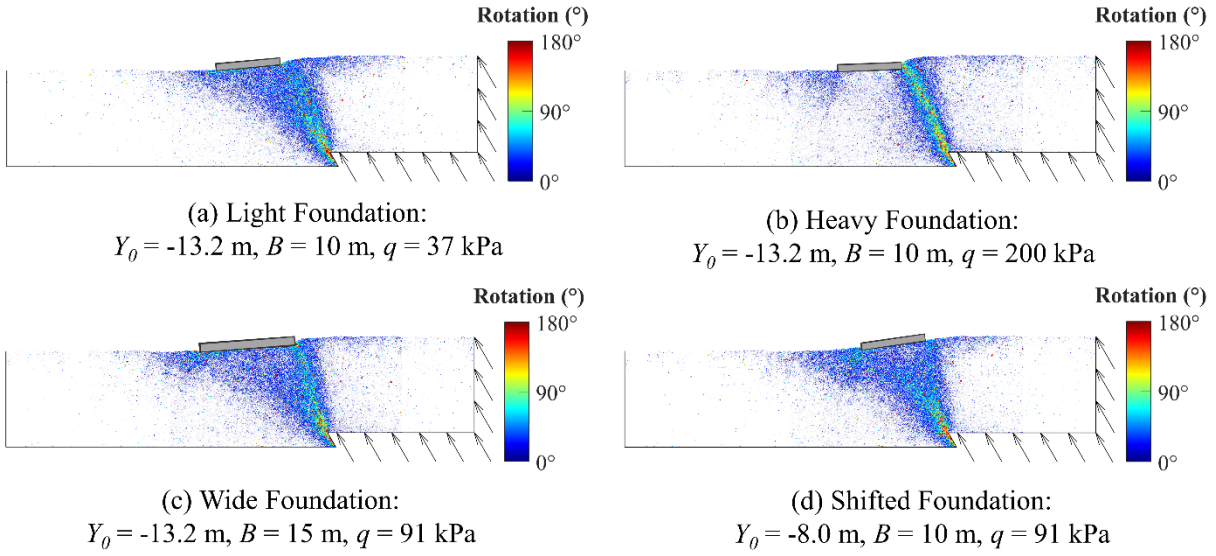

Figure 2. Fault rupture development shown in terms of clump rotations for select FR-SFI cases.

4 CONCLUSIONS

The FR-SFI simulations of this study show that DEM has potential to provide much insight into the interaction between a propagating fault rupture surface and a rigid foundation that cannot be captured using more commonplace continuum methods. The simulations showed that heavy foundations tend to undergo much less rotation than lighter foundations equivalently located during reverse FR-SFI and that cases that produce more shear activity beneath the foundation tend to cause the foundation to undergo more rotation. While the insights provided by DEM are elucidated thoroughly with the high-performance computing simulations of Garcia & Bray (2019), the simulations performed in this study using fewer particles with *PFC3D* are qualitatively similar to their findings. Thus, *PFC3D* can be a viable tool for qualitatively understanding mechanisms of FR-SFI through parametric analysis of the effect of foundation shape, size, and weight.

REFERENCES

Anastasopoulos, I., Callerio, A., Bransby, M. F., Davies, M. C. R., El Nahas, A., Faccioli, E., Gazetas, G., Masella, A., Paolucci, R. & Rossignol, E. 2008. Numerical analyses of fault–foundation interaction. *Bull. of Earthquake Eng.*, 6(4), 645-675.

Anastasopoulos, I., Antonakos, G. & Gazetas, G. 2010. Slab foundation subjected to thrust faulting in dry sand: Parametric analysis and simplified design method. *Soil Dyn. and Earthq. Eng.*, 30(10), 912-924.

Bransby, M. F., Davies, M. C. R., El Nahas, A. & Nagaoka, S. 2008b. Centrifuge modeling of reverse fault-foundation interaction. *Bull. Earthquake Eng.*, 6(4), 607–628.

Bray, J. D. 2001. Developing Mitigation Measures for the Hazards Associated with Earthquake Surface Fault Rupture. In *A Workshop on Seismic Fault-Induced Failures – Possible Remedies for Damage to Urban Facilities, Research Project 2000 Grant-in-Aid for Scientific Research* (No. 12355020), Japan Society for the Promotion of Science, Workshop Leader, Kazuo Konagai, University of Tokyo, Japan, pp. 55-79, January 11-12, 2001 [Invited Paper].

Garcia, F.E. & Bray, J.D. 2018a. Distinct element simulations of shear rupture in dilatant granular media. *Int. J. of Geomechanics*, 18(9), 04018111.

Garcia, F.E. & Bray, J.D. 2018b. Distinct Element Simulations of Earthquake Fault Rupture through Materials of Varying Density. *Soils and Foundations*, V. 58, doi.org/10.1016/j.sandf.2018.05.009.

Garcia, F.E. & Bray, J.D. 2019. Discrete element analysis of earthquake fault rupture-soil-foundation interaction. *J. of Geotech. and Geoenviron. Eng.*, 145(9), 04019046.

Itasca Consulting Group, Inc. 2014. *PFC3D – Particle Flow Code in 3 Dimensions, Ver. 5.0*. Minneapolis: Itasca.

Niccum, M. R., Cluff, L. S., Chamoro, F. & Wylie, L. 1976. Banco Central de Nicaragua: a case history of a highrise building that survived surface fault rupture. In C. B. Humphrey (ed), *Engineering geology and soils engineering symposium*, Vol. 14, 133-144. Idaho Department of Transportation, Division of Highways, Boise, ID.

Oettle, N. & Bray, J.D. 2013a. Fault Rupture Propagation through Previously Ruptured Soil. *J. of Geotechnical and Geoenvironmental Engineering*, ASCE, 139(10), 1637-1647, DOI: 10.1061/(ASCE)GT.1943-5606.0000919.

Oettle, N. & Bray, J.D. 2013b. Geotechnical Mitigation Strategies for Earthquake Surface Fault Rupture. *J. of Geotechnical and Geoenvironmental Engineering*, ASCE, 139(11), 1864-1874, DOI:10.1061/(ASCE)GT.1943-5606.0000933.

Oettle, N.K. & Bray, J.D. 2016. Numerical Procedures for Simulating Earthquake Fault Rupture Propagation. *Inter. J. of Geomech.*, 17(1), 04016025.

Stirling, M.W., Litchfield, N.J., Villamor, P., Van Dissen, R.J., Nicol, A., Pettinga, J., ... & Mountjoy, J. 2017. The Mw 7.8 2016 Kaikōura earthquake: Surface fault rupture and seismic hazard context. *Bull. New Zeal. Soc. Earthq. Eng*., (2), 73-84.